Hybrid Density Functional Studies of a Bacteriopheophytin *a* Model and Its Anion Radical Form: Geometry, Spin Densities, and Hyperfine Couplings

PATRICK J. O'MALLEY

Department of Chemistry, UMIST, Manchester, M60 1QD, United Kingdom

Received 25 January 1999; accepted 10 April 1999

ABSTRACT: Hybrid density functional calculations are performed on models of the bacteriopheophytin *a* molecule, which acts as an electron acceptor in the initial electron transfer events of bacterial photosynthesis. The geometry of the neutral and one-electron reduced free radical form are calculated. Little variation in the main π framework geometry is predicted to occur on one-electron reduction. The electron density of the SOMO for the anion free radical form is also investigated, and the unpaired spin density distribution is also analyzed. Anisotropic and isotropic hyperfine couplings are calculated and discussed on the basis of the unpaired spin density distributions. The electron density of the SOMO is shown to extend on to the carbonyl group attached to ring A; the extent of this delocalization being dependent on the twist angle, this group makes with the main ring plane with the magnitude of the ^{1}H hyperfine couplings of the 2^{1} methyl group strongly dependent on the value of this twist angle. Good agreement is observed between calculated and experimentally measured isotropic hyperfine couplings. © 1999 John Wiley & Sons, Inc. J Comput Chem 20: 1292–1298, 1999

Keywords: hybrid density functional calculations; bacteriopheophytin *a*; geometry; spin densities; hyperfine couplings

Correspondence to: P. J. O'Malley; e-mail: patrick@trigger.ch.umist.ac.uk

CCC 0192-8651 / 99 / 121292-07

Introduction

Pheophytin molecules play a crucial role in the electron transfer reactions of higher plant and photosynthetic bacteria. In purple photosynthetic bacteria and Photosystem II of higher plants and algae, a (bacterio)pheophytin molecule acts as an early acceptor of an electron forming a (bacterio)pheophytin anion radical. The three-dimensional structures of the bacterial and higher species photosynthetic reaction centers[1–3] are now furnishing details of the spatial structure of these important molecules in their *in vivo* environment. A full understanding of electron transfer requires both the spatial and electronic structures for the electron transfer pigments involved. EPR spectroscopy, via the nuclear electron hyperfine couplings, can furnish partial information concerning the electronic structure of the one-electron reduced free radial forms of these pigments. The information obtained is often limited, however, to proton hyperfine interactions, which are indirectly related to the one-electron wavefunction of the unpaired electron. The more desirable ^{13}C isotropic and particularly the anisotropic hyperfine couplings often present insurmountable experimental difficulties.

Density functional methods, using the B3LYP functional, are the method of choice for studying the electronic properties of medium- to large-sized free radicals.[4–6] In this study we concentrate on models for the bacteriopheophytin *a* molecule, which act as an electron acceptor in the reaction centers of purple bacteria. The model permits us to compare optimized geometries for neutral and the one-electron reduced anion radical form, which is infeasible for the more highly substituted forms found *in vivo*. In such a fashion we can examine any structural changes predicted to occur to the main π framework on reduction. Analysis of the electron density of the SOMO orbital is used to predict the extent of the wavefunction of the unpaired electron. Unpaired spin density (alpha-beta) distributions and isotropic and anisotropic hyperfine couplings are also calculated and discussed.

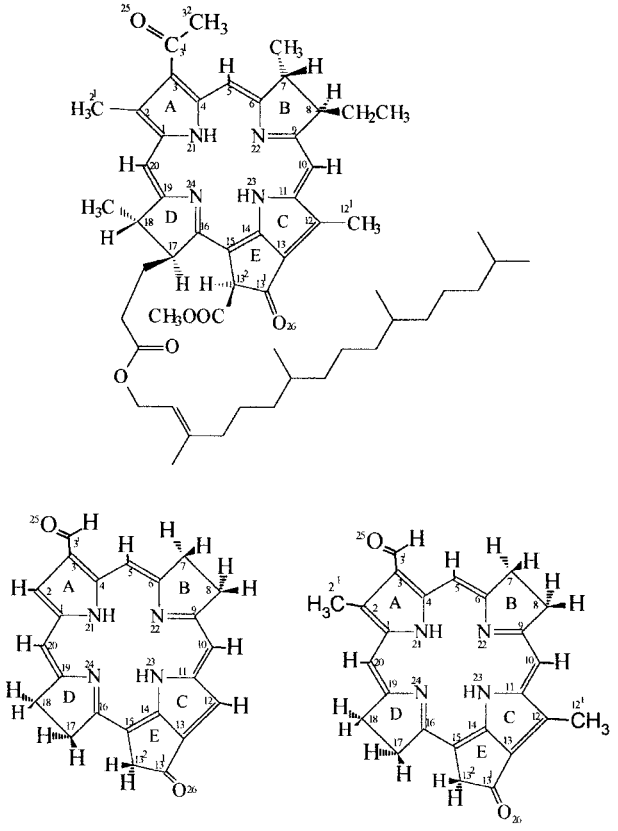

FIGURE 1. Top, bacteriopheophytin *a*. Bottom, BPh-0 (left) and MeBPh-0 (right), models used in calculations, C_s symmetry.

Methods

The bacteriopheophytin *a* molecule is shown in Figure 1, together with the models used in this study. In the two models, termed BPh-0 and MeBPh-0, the main π framework is retained. Peripheral substituent groups, which do not contribute to the frontier orbitals, have been omitted.

All density functional calculations were performed using the Gaussian 94 electronic structure code.[7] All calculations were performed at the unrestricted Kohn–Sham level with the hybrid functional B3LYP. The isotropic and anisotropic hyperfine couplings were calculated as described in ref. 4. For geometry optimization and anisotropic hyperfine coupling determination the 6-31G(d) basis set was employed, while the larger EPR-II basis set was employed for isotropic hyperfine coupling calculations on the larger MeBPh models. Graphical generation of electron density isosurfaces was achieved using the SPARTAN package.[8]

Results and Discussion

The numbering scheme is given in Figure 1. For BPh, the principal bond lengths and angles are compared in Figures 2 and 3 for the neutral and

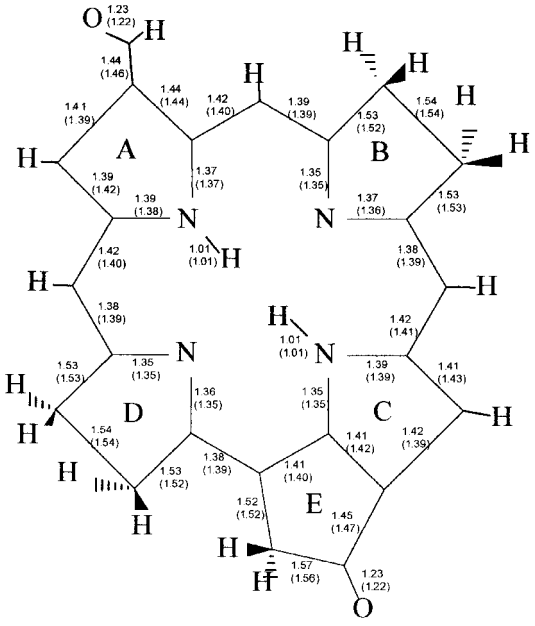

FIGURE 2. Selected bond distances for one electron reduced and neutral (brackets) BPh-0 forms. Values given in angstroms. Molecule orientation as in Figure 1.

the one-electron reduced anion radical. Essentially no significant geometrical changes are brought about by reduction of the neutral form. This is important for electronic structure studies of the *in vivo* forms as it indicates that geometrical data

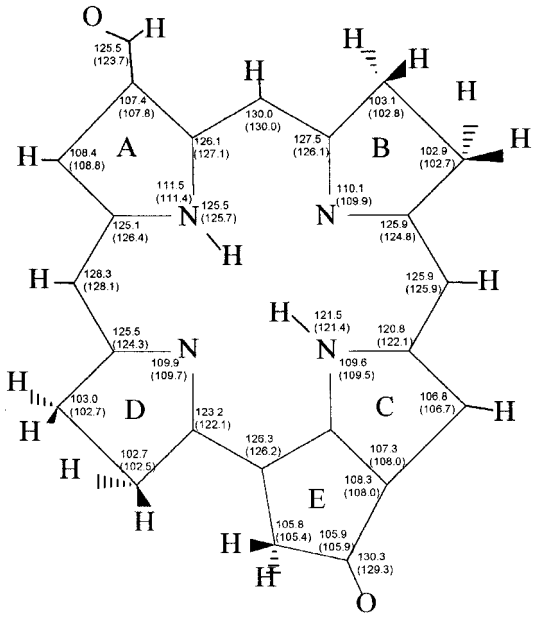

FIGURE 3. Selected bond angles for one-electron reduced anion radical and neutral (brackets) BPh-0 forms. Values given in degrees. Molecule orientation as in Figure 1.

obtained, by X-ray structure analysis[1–3] for the neutral state could be used for calculations on the anion radical form. The absence of structural changes on reduction is also suggestive of low reorganizational energy associated with one-electron capture. According to the Marcus theory of electron transfer,[9] this will contribute to the fast picosecond electron transfer observed for bacteriopheophytin reduction in the photosynthetic reaction center.

The SOMO(alpha HOMO) electron density isosurfaces for the anion free radical form, BPh-0 are shown in Figure 4. The three contours demonstrate that the electron density is concentrated at the N22, N24, O25, and O26 atom positions. Significant electron density is also found at the C2, C3, C5, C10, C12, C15, and C20 positions. In EPR/ENDOR hyperfine coupling studies the interaction of the nuclear spin with the unpaired spin density is measured. While to a first approximation the unpaired spin density will correspond to the electron density of the SOMO, spin polarization effects caused by the exchange interaction between electrons of similar spin will alter this somewhat; a principal effect is the introduction of regions of negative (excess beta) spin density within the radical. This is illustrated in Figure 5, where the unpaired spin density is represented by different contours. The positive spin density contours are similar to the electron density plots for the SOMO, as they reflect regions of excess alpha spin. The negative spin density surface shows how spin po-

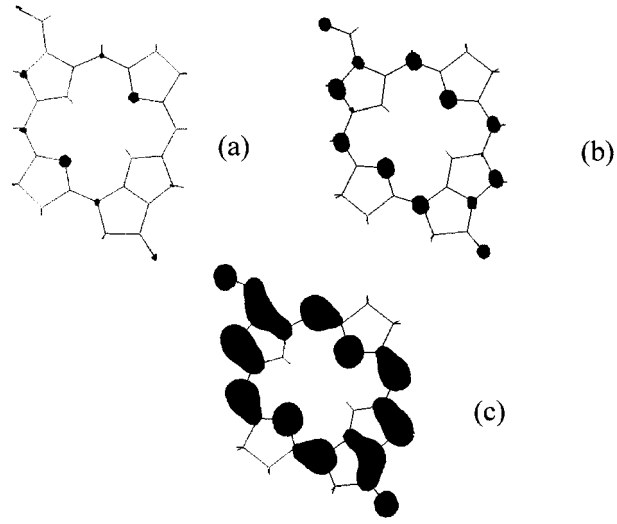

FIGURE 4. SOMO electron density distributions for BPh-0. (a) 0.10 e/au^3, (b) 0.07 e/au^3, and (c) 0.03 e/a^3. Molecule orientation as in Figure 1.

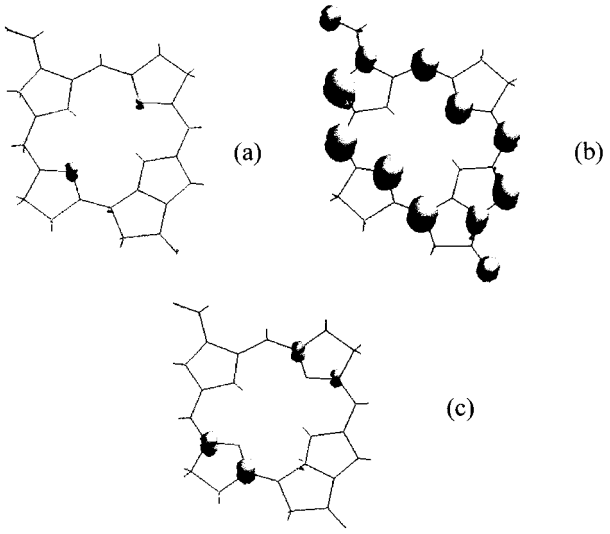

FIGURE 5. Unpaired spin density isosurfaces for BPh-0. (a) 0.02 e/au^3, (b) 0.003 e/au^3, and (c) −0.003 e/au^3. Molecule orientation as in Figure 1.

larization introduces excess beta spin in nodal regions of the SOMO. The centers having the most negative negative spin density are C6, C9, C16, and C19. The anisotropic hyperfine couplings calculated and presented in Tables I, II, and III provide a more quantitative measure of these spin density distributions, and are, of course, at least in principle, measurable by electron paramagnetic resonance spectroscopy. As can be predicted from the spin density contours shown in Figure 5, the magnitude of the principal anisotropic hyperfine coupling values is largest for positions C2, C5, C10, C15, C12, C13, C15, and C20. Large magnitude values are also found for the N22 and N24 nitrogens and the two oxygens, O25 and O26. The relative magnitude of the anisotropic tensor values can indeed by predicted from the extent of the spin density contours. For example, the larger anisotropic principal hyperfine tensor values for N24 compared with N22 could be predicted from the extent of the 0.02 e/au^3 spin density contour in Figure 5a. Regions containing negative unpaired spin density results, as expected, in a reversal of the sign of the major anisotropic tensor component. This is demonstrated by the C16 and C19 values in Table IV. Here, again, the order in magnitude demonstrated by the anisotropic principal values, i.e., C9 < C6 < C19 < C16 is reflected in the extent of the spin density contours of Figure 5c.

From the high resolution structures of the bacterial reaction centers so far, a notable structural

TABLE I.
^{13}C Anisotropic (T) Hyperfine Couplings Calculated for C1 to C10.

Atom	BPh-0	BPh-45	BPh-90
	T_{11}	T_{11}	T_{11}
	T_{22}	T_{22}	T_{22}
	T_{33}	T_{33}	T_{33}
C1	0.5	2.6	5.0
	0.5	−0.6	−1.9
	−1.0	−2.0	−3.1
C2	23.0	19.7	14.1
	−11.3	−9.7	−7.0
	−11.7	−10.0	−7.1
C3	8.2	10.0	13.7
	−3.7	−4.7	−6.8
	−4.5	−5.2	−6.9
C3^1	2.9	2.0	0.5
	−1.0	−0.6	−0.2
	−1.9	−1.4	−0.3
C4	0.6	2.7	5.8
	−0.2	−0.9	−2.3
	−0.4	−1.8	−3.5
C5	15.5	16.0	17.6
	−7.6	−7.9	−8.7
	−7.9	−8.1	−8.9
C6	3.3	3.1	2.7
	1.8	1.5	1.0
	−5.2	−4.6	−3.7
C7	0.2	0.2	0.2
	0.0	−0.1	−0.1
	−0.2	−0.2	−0.1
C8	0.2	0.2	0.2
	0.0	0.0	0.0
	−0.1	−0.2	−0.2
C9	2.5	3.0	4.0
	1.2	1.6	2.3
	−3.8	−4.6	−6.4
C10	13.3	14.5	17.1
	−6.6	−7.2	−8.4
	−6.7	−7.3	−8.7

All values given in MHz.

difference found for two bacteriopheophytin molecules present is the different rotational angle (with respect to the main ring plane) of the acetyl group attached to ring A, a formyl group in our model. In the *Rb sphaeroides* reaction center[1] the bacteriopheophytin *a* molecule, along the active A branch of electron transfer, has this group twisted out of the main ring plane giving rise to an O25C3^{1}C3C2 dihedral angle of 37 degrees. For the other bacteriopheophytin *a* molecule, found along the inactive B branch, this twist angle is 66 degrees. It is apparent from the electron density of

TABLE II.
^{13}C, Anisotropic (T) Hyperfine Couplings Calculated for C11 to C20.

Atom	BPh-0	BPh-45	BPh-90
	T_{11}	T_{11}	T_{11}
	T_{22}	T_{22}	T_{22}
	T_{33}	T_{33}	T_{33}
C11	3.2	2.5	1.3
	−1.0	−0.7	0.0
	−2.2	−1.9	−1.3
C12	14.7	15.4	17.0
	−7.2	−7.6	−8.3
	−7.5	−7.8	−8.6
C13	10.5	10.3	9.8
	−4.9	−4.8	−4.5
	−5.6	−5.5	−5.3
$C13^1$	2.2	2.4	2.7
	−0.4	−0.5	−0.7
	−1.8	−1.9	−2.0
C14	2.3	2.2	2.0
	−1.8	1.7	1.5
	−4.1	−3.9	−3.6
C15	24.1	23.6	22.4
	−11.8	−11.6	−11.0
	−12.3	−12.0	−11.4
C16	6.1	6.0	5.7
	4.1	4.0	3.8
	−10.2	−10.0	−9.5
C17	0.3	0.3	0.3
	−0.1	−0.1	−0.1
	−0.3	−0.3	−0.3
C18	0.3	0.3	0.3
	−0.1	−0.1	−0.2
	−0.2	−0.2	−0.2
C19	5.5	4.9	4.1
	3.4	2.9	2.2
	−8.9	−7.7	−6.4
C20	24.2	23.2	21.4
	−11.9	−11.4	−10.6
	−12.3	−11.7	−10.8

All values given in MHz.

TABLE III.
^{14}N and ^{17}O Anisotropic (T) Hyperfine Couplings.

Atom	BPh-0	BPh-45	BPh-90
	T_{11}	T_{11}	T_{11}
	T_{22}	T_{22}	T_{22}
	T_{33}	T_{33}	T_{33}
N21	0.5	0.6	0.7
	0.5	0.6	0.7
	−1.0	−1.2	−1.5
N22	9.3	9.9	11.4
	−4.6	−4.9	−5.7
	−4.7	−5.0	−5.8
N23	0.3	0.3	0.3
	0.3	0.3	0.3
	−0.5	−0.5	−0.6
N24	14.4	14.1	13.6
	−7.1	−7.0	−6.7
	−7.3	−7.2	−6.9
O25	−13.5	−9.7	−1.1
	6.7	4.8	0.5
	6.8	4.9	0.5
O26	−17.5	−17.5	−17.6
	8.8	8.7	8.8
	8.8	8.8	8.8

All values given in MHz.

the SOMO in Figure 4 that this group forms part of the conjugation pathway for this frontier orbital. As such variations in this structural feature can be expected to change the properties (in particular, spin densities and electron affinity) of the molecule significantly, in this study we have rotated the formyl group out of the main ring plane by 45(BPh-45) and 90(BPh-90) degrees to examine the effect of such orientations on the electron densities and hyperfine couplings. The SOMO for the BPh-0, BPh-45, and BPh-90 are illustrated in Figure 6. In BPh-0 the SOMO electron density extends out on to the formyl group in a similar fashion to that observed for the ring E carbonyl group. As the plane of the formyl group is progressively moved out of the main ring plane this delocalization is progressively decreased, and the electron density that extended out on to the formyl group now builds up at ring A. A more quantitative measure of these effects can be obtained from the anisotropic hyperfine coupling constants for each nuclei of the radical. The anisotropic hyperfine couplings are directly proportional to the spin density surrounding each nucleus. The symmetry aspects of the tensor principal values will depend on the shape of this spin density. The anisotropic hyperfine couplings are presented in Tables I–III. The principal effect of the formyl group rotation can be discerned as a decrease in the absolute magnitude of the O25 $C3^1$ and C2 hyperfine values in going from BPh-0 to BPh-90. The absolute magnitude of the C1, C4, and C3 values show a corresponding increase. Small variations are found for other nuclei removed from ring A. These changes reflect the alteration of the SOMO electron density referred to above. Essentially, rotating the group out of the main ring plane stems the SOMO electron density flow on to the formyl group nuclei. As such, the anisotropic hyperfine coupling for the

TABLE IV.
^{14}N and ^{1}H Calculated Isotropic Hyperfine Couplings for MeBPh Compared with Experimental (10) Determinations for Bacteriopheophytin *a*.

Atom	MeBPh-0 A_{iso}	MeBPh-45 A_{iso}	MeBPh-90 A_{iso}	Expt A_{iso}
N21	−0.9	−1.2	−1.8	−1.2
N22	4.5	4.7	5.5	6.2
N23	−0.6	−0.5	−0.6	−0.6
N24	7.9	7.7	7.5	7.2
$CH_3(2^1)$	9.6	7.8	5.7	7.1, 8.3
$CH_3(12^1)$	5.8	6.0	6.6	
H5	−5.9	−6.2	−6.9	−6.9, −8.0, −8.5
H10	−5.1	−5.5	−6.7	
H20	−11.0	−10.6	−9.9	

For methyl groups, an average value for a static orientation of the three hydrogens is presented. All values given in MHz.

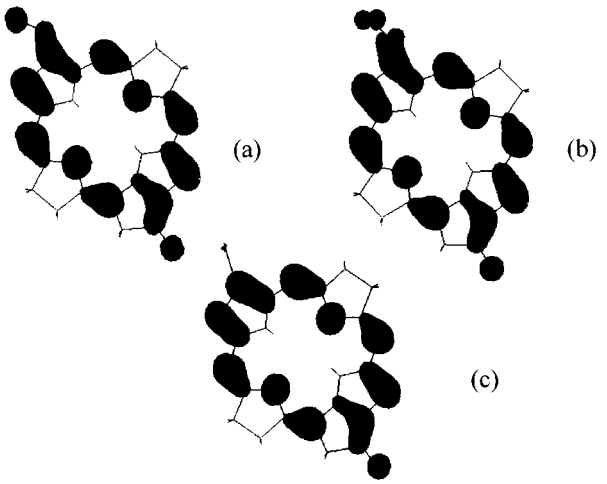

FIGURE 6. SOMO electron density isosurfaces (0.03 e/au^3) for (a) BPh-0, (b) BPh-45, and (c) BPh-90. Molecule orientation as in Figure 1.

formyl group are decreased, and correspondingly, the buildup of spin density on ring A for the 45 and 90 degree forms results in an increased magnitude of the anisotropic hyperfine couplings for the C3 and C4 nuclei. Of particular note is the decrease in the hyperfine coupling of the C2 nucleus for increasing angle. This decrease can be mainly attributed to spin polarization by increasing alpha spin on C3, i.e., as the formyl group is progressively moved out of the main ring there is increasing alpha spin at the C3 position (Fig. 4). Due to spin polarization, this will give rise to more beta spin at the neighboring C2 position, thereby reducing the unpaired spin (alpha-beta) at this position.

So far, experimental EPR and ENDOR/TRIPLE studies of the bacteriopheophytin *a* anion radical have been able to obtain isotropic hyperfine couplings for the four nitrogen atom positions and also for some of the main ring hydrogens.[10,11] The methyl groups attached to the 2^1 and 12^1 positions are particularly amenable to ENDOR studies for both *in vitro* and *in vivo* radicals, and so far comparison with experimental data we use the extended model shown in Figure 2c. As stated in the Methods section, we also use the more extended EPR-II basis set, which is optimized for isotropic hyperfine coupling prediction. The calculated isotropic hyperfine couplings are compared with experimental determinations in Table IV.

Considering the approximations inherent in the model studied, the quantitative agreement between experimental and calculated values is highly satisfactory. As expected, the trends in spin density and anisotropic hyperfine couplings reported above are reproduced by the isotropic hyperfine data. Of particular note are the values for the 2^1 and 12^1 methyl group hydrogens. The value of the 2^1 group shows a significant decrease as the formyl group is moved out of the main ring plane, showing a 40% decrease in magnitude when the formyl group is perpendicular to the main ring plane. The ^{1}H isotropic hyperfine coupling value of the 12^1 methyl group shows a corresponding but smaller increase, increasing by 14% for the perpendicular orientation of the formyl group. As the spin density at the methyl group hydrogens arises due to hyperconjugation with the main π system these trends exactly mimic the variation in the ^{13}C anisotropic hyperfine coupling values for the 2 and 12 positions discussed above, which can be traced back to the decrease in conjugation of the SOMO onto the formyl group as it progressively rotated out of the main ring plane. In the protein environment the orientation of the acetyl group plane will

be determined by nonbonding interactions with the immediate environment such as Van der Waals forces and hydrogen bonding. Recent ENDOR/TRIPLE studies of the bacteriopheophytin *a* anion radical in vivo[11] have indeed shown that the isotropic hyperfine coupling values for the 2^1 and 12^1 methyl groups differ, depending on sample preparation and mutant species studied. As this study has demonstrated, different orientations of the acetyl group on ring *a* are the most likely reasons for such variations.

Conclusions

Hybrid density functional calculations utilizing the B3LYP function give important information on the properties of bacteriopheophytin *a*. Minute variation in the main π framework geometry is predicted to occur on one-electron reduction. The electron density of the SOMO of the anion radical is shown to extend on to the carbonyl group attached to ring A; the extent of this delocalization being dependent on the twist angle, this group makes with the main ring plane. Calculated isotropic and anisotropic hyperfine couplings are shown to be particularly sensitive to this geometrical feature.

References

1. Ermler, U.; Fritzsch, G.; Buchanan, S. K.; Michel, H. Structure 1994, 2, 925.
2. Stowell, M. H. B.; McPhillips, T. M.; Rees, D. C.; Soltis, S. M.; Abresch, E.; Feher, G. Science 1997, 276, 812.
3. Lancaster, C. R. D.; Michel, H. Structure 1997, 5, 1339.
4. (a) O'Malley, P. J. J. Phys Chem A 1997, 101, 6334; (b) O'Malley, P. J. J. Phys Chem A 1997, 101, 6334; (c) O'Malley, P. J.; Ellson, D. A. Biochim Biophys Acta 1997, 1320, 65.
5. (a) Barone, V. In Recent Advances in Density Functional Methods; Chong, D. P., Ed.; World Scientific Publishing: Singapore, 1995; (b) Rega, N.; Cossi, M.; Barone, V. J. Am Chem Soc 1998, 120, 5723.
6. Himo, F.; Grasslund, A.; Eriksson, L. E. Biophys J 1997, 72, 1556.
7. Frisch, M. J.; Trucks, G. W.; Schlegel, H. B.; Gill, P. W.; Johnson, B. G.; Wong, M. W.; Foresman, J. B.; Robb, M. A.; Head–Gordon, M.; Replogle, E. S.; Gomperts, R.; Andres, J. L.; Raghvachari, K.; Binkley, J. S.; Gonzalez, C.; Martin, R. L.; Fox, D. J.; Defrees, D. J.; Baker, J.; Stewart, J. J. P.; Pople, J. A. GAUSSIAN 94 Gaussian Inc.; Pittsburgh: PA, 1995.
8. SPARTAN 5.1; Wavefunction Inc.; Irvine, CA, 1997.
9. Marcus, R. A. Annu Rev Phys Chem 1964, 15, 155.
10. Lubitz, W.; Lendzian, F.; Moebius, K. Chem Phys Lett 1981, 84, 33.
11. Mueh, F.; Williams, J. C.; Allen, J. P.; Lubitz, W. Biochemistry 1998, 37, 13066.